Modeling of solute transport in snow using conservative tracers and artificial rain-on-snow experiments

Jeonghoon Lee,[1] Xiahong Feng,[1] Eric S. Posmentier,[1] Anthony M. Faiia,[1] Randall Osterhuber,[2] and James W. Kirchner[3]

Received 29 August 2006; revised 11 September 2007; accepted 2 October 2007; published 6 February 2008.

[1] We report a study of solute transport in snow, using artificial rain-on-snow experiments with conservative anions (F^-, Br^-, and SO_4^{2-}). The tracers were mixed into tap water and sprayed onto the snow surface from two water supply tanks. The water flux out of the base of the snowpack was recorded, and discharge samples were collected and analyzed for the three tracers. The chemical concentration of tracers in the discharge was negatively associated with the water flux. The objectives of the experiment were to test whether the mobile-immobile model (MIM) with variable mobile-immobile water exchange coefficient can simulate both positive and negative concentration-discharge relationships in this and previous tracer experiments. By simulating our experimental data, we confirm that it is necessary for the exchange coefficient to increase with water velocity. In addition, we use the model to show that with a diurnal variation of clean water flux, a negative concentration-discharge relationship occurs when solutes are evenly distributed in the mobile and immobile fluids, while a positive relationship occurs when the solutes were present only in the immobile fluid near the surface. This result may help in explaining the complicated concentration-discharge relationships observed in catchments.

Citation: Lee, J., X. Feng, E. S. Posmentier, A. M. Faiia, R. Osterhuber, and J. W. Kirchner (2008), Modeling of solute transport in snow using conservative tracers and artificial rain-on-snow experiments, *Water Resour. Res.*, *44*, W02411, doi:10.1029/2006WR005477.

1. Introduction

[2] Snowmelt from seasonal snowpacks is important for producing spring stream discharge in northern and alpine environments [*Singh et al.*, 1997] and is the dominant fresh water source in some areas. During the snowmelt season, solutes (such as H^+, NO_3^-, SO_4^{2-}, etc.) that have been accumulated in the snowpack throughout the winter are released [*Tranter et al.*, 1986]. The magnitude and timing of the solute release depends on how solutes are eluted from the pore water between snow grains [*Harrington et al.*, 1996; *Harrington and Bales*, 1998; *Feng et al.*, 2001]. An exponential decrease of solute concentrations (i.e., an ionic pulse) has been reported through the melting season [*Johannesssen and Henriksen*, 1978], and so have diurnal variations that were negatively associated with the melting rate [*Bales et al.*, 1989; *Williams and Melack*, 1991]. This negative concentration-discharge relationship was explained as a result of dilution by clean meltwater at high melting rates.

[3] *Hibberd* [1984] simulated the ionic pulse using a standard advection-dispersion model. This model was unable to simulate the long tail following initial solute arrival. This limitation was overcome by the mobile-immobile model (MIM) which simulates preferential flow in snow [e.g., *Harrington and Bales*, 1998]. The MIM partitions water into mobile and immobile fractions. Mobile water transports solutes by advection and dispersion, whereas immobile water does not flow, but exchanges its solute with the mobile water following first-order kinetics. *Harrington and Bales* [1998] used a numerical solution to the flow and solute transport equations in a MIM with a fixed mobile-immobile water exchange rate coefficient, and simulated both the flow caused by snowmelt and the solute concentrations of the meltwater. Their MIM also reproduced the negative relationship between solute concentration and flow rate.

[4] Using rare earth element tracers and rain-on-snow storms, *Feng et al.* [2001] reported a positive relationship between tracer concentration and discharge. They argued that the MIM with a fixed exchange rate coefficient could not reproduce their observations, in which the tracer concentration increased with increasing discharge. By allowing the exchange rate coefficient to increase with the effective water content in an MIM model that was fed by analytic solutions of meltwater flow model, they successfully explained both their experimental observations of positive relationships between solute concentration and flow rate under certain conditions, and negative relationships under others.

[5] This study was designed to test further the necessity of having a flow-dependent exchange rate coefficient as proposed by *Feng et al.* [2001] under different hydrological and chemical conditions. Artificial rain-on-snow storms were generated over a natural snowpack. The most important

[1]Department of Earth Sciences, Dartmouth College, Hanover, New Hampshire, USA.
[2]Central Sierra Snow Laboratory, Soda Springs, California, USA.
[3]Department of Earth and Planetary Science, University of California, Berkeley, California, USA.

0043-1397/08/2006WR005477$09.00

experimental difference between this experiment and *Feng et al.* [2001] is that chemical tracers were introduced by artificial rainwater as mobile water rather than prior to rainstorms as immobile water. Conservative tracers (F^-, Br^- and SO_4^{2-}) were used to avoid the possibility of adsorbing onto dust particles in snow which is a concern with rare earth elements. We combined the solute transport model of *Feng et al.* [2001] and a numerical flow model in order to realistically simulate the water flow and link the solute transport with rainfall and melting rates. This combined model allows us to investigate how hydrological conditions affect the exchange rate coefficient, and to explore concentration-discharge relationships under various chemical conditions.

2. Site Information and Experimental Description

2.1. Field Site

[6] The study was carried out at the Central Sierra Snow Laboratory (CSSL), which is located at 39°22′19.5″N, 122°22′15″W, and at an altitude of 2100 m on the southwest crest of the Sierra Nevada near Soda Springs, California, USA. The average annual precipitation, snowfall, and peak snow depth are 1.3, 10.4, and 2.4 m, respectively. The mean yearly maximum and minimum air temperatures are 26 and −10°C. On average, the site receives ~80% of its precipitation in the form of snow. The snow laboratory is instrumented to measure meteorological variables, including shortwave radiation. There are two 6 × 3 m^2 melt pans sloped gently to corner drains. The discharge from each melt pan is measured by a 4-L datalogging tipping bucket.

2.2. Artificial Rain-on-Snow Experiments

[7] We conducted two artificial rain-on-snow experiments on 5 and 8 April 2003. During the winter of 2002–2003, the total precipitation (from 1 November 2002 to 31 May 2003) was 1454 mm, of which 74% was snow. The depth of snowpack prior to the experiments was 210 cm. During the time period of observation, the air temperature ranged from −5 to 12°C, remaining below zero all day on 5, 6, 12, and 13 April.

[8] The artificial rainstorms were generated with two lawn sprinklers, placed about 6 m apart opposite each other along the bisector of the length of the snow pan. The inundated area was thus double the width of the pan. Tap water was pumped to the sprinklers from two water supply tanks dug into the snow and lined with plastic sheets. Conservative chemical tracers, F^- (KF) and Br^- (LiBr), were mixed into the tanks for the first and second rain-on-snow experiments, respectively, and a sample of the tank water was taken to measure the tracer concentrations in the artificial rainwater. The tap water used to fill the tanks contained a substantial amount of sulfate (~9.4 mg/L), which was significantly higher than the baseline concentration in the snow. Therefore sulfate, as well, is treated as a chemical tracer in this work. The water temperature of the tap water used to prepare the tracer solutions was 1°C. The actual water sprayed onto the snow surface may have been colder because of cooling in the water tanks. However, no freezing occurred in the tanks.

[9] To measure the rainfall amount, we placed 20 plastic cups distributed over the snow surface to collect precipitation. At the end of each rain event, the water in the cups was weighed, and averaged. The first experiment was performed in the afternoon of 5 April; the rainfall lasted 5.1 hours and the amount of rainfall was 157 ± 15 mm (±1σ, among the 20 cups). The second storm was on the morning of 8 April, and lasted 5.5 hours with 145 ± 8.5 mm of precipitation. There was no natural rainfall during the artificial storm periods, but 10 cm of snow fell on 12 and 13 April.

[10] To obtain the prestorm chemistry and physical properties for the snowpack, we dug a pit in an adjacent area, and measured snow temperature, density and water content throughout the profile. Density was measured by weighing 1000 cm^3 of snow. The snow samples were then transferred to precleaned (with Citronox®) plastic bags, melted, and transferred to precleaned plastic bottles and kept refrigerated until they were analyzed for F^-, Br^- and SO_4^{2-} concentrations. Liquid water content was measured with a snow surface dielectric device (Denoth meter). The area next to the pit was sprayed with F^- containing water for 5.3 hours with 135 ± 2.0 mm of precipitation. The snow temperature, density and water content under the spayed area were measured after this storm. The same area was sprayed by a second storm containing Br^- for 5.2 hours with 142 ± 2.7 cm of precipitation, following which the snow temperature, density and water content were again measured.

2.3. Sampling and Chemical Analyses

[11] At user-defined intervals, a custom meltwater sampling system pumped ~125 mL of meltwater from the north pan upstream of the tipping bucket into a precleaned plastic bottle on a rotating tray. The absolute sampling times were recorded by an event data logger. We sampled the melt-pan discharge every 12 min after the onset of the first storm (5 April) and reduced the sampling frequency during low flow to every 90 min on 6 and 7 April. The sampling rate was again increased to every 15 min during and after the second storm (8 April), and then decreased to every hour on 10 and 11 April, and every 2 hours on and after 12 April.

[12] All samples, including the tap water, the snow profile samples, the artificial rainwater containing the tracers, and the samples from the melt pan discharge, were analyzed for F^-, Br^-, and SO_4^{2-} concentrations using an Ion Chromatography (IC) (Dionex) system. Standards were run for about every 10 samples. The relative standard deviation of the analyses is within 2%.

2.4. Numerical Modeling

2.4.1. Mathematical Model

[13] A 1-D (vertical) numerical model was developed by combining the numerical solute transport model of *Feng et al.* [2001] and a numerical solution of the flow equation (3) from *Colbeck* [1972] in order to simulate the water flow and link the solute transport with rainfall and melting rates.

[14] The volumetric flux q_z of meltwater is given by *Colbeck* [1972] as

$$q_z = KS^n, \tag{1}$$

where S is the effective water saturation (see Table 1 for definitions of variables) and n is an empirical exponent. K is hydraulic conductivity for saturated flow,

$$K = \frac{\rho_w \cdot k \cdot g}{\mu}, \tag{2}$$

Table 1. Snowpack Properties and Symbols Used in This Study

Symbol	Meaning (Values Used in the Simulations If Not Otherwise Specified)	Units	Dimension
a	total mass of water per unit snow volume	g cm^{-3}	g of total water/cm^3 snow
a_i	mass of immobile water per unit snow volume	g cm^{-3}	g of immobile water/cm^3 snow
a_m	mass of mobile water per unit snow volume	g cm^{-3}	g of mobile water/cm^3 snow
b	mass of ice per unit snow volume	g cm^{-3}	g of ice/cm^3 snow
C_i	tracer concentration in immobile phase	g/cm^{-3}	g of solute mass/cm^3 of immobile water
C_{ice}	initial concentration in ice ($C_{ice} = 0$)	g/cm^{-3}	
C_m	tracer concentration in mobile phase	g/cm^{-3}	g of solute mass/cm^3 of mobile water
C_r	tracer concentration when sprayed	g/cm^{-3}	g of solute mass/cm^3 of water
D	dispersion coefficient	cm^2/h	
d	dynamic dispersivity ($d = 0.05$)	cm	
g	gravitational acceleration	cm h^{-2}	
K	hydraulic conductivity	cm h^{-1}	
k	intrinsic permeability	cm^2	
n	exponent		3
q_z	specific discharge	cm h^{-1}	$q_z = KS^3$ cm of snow × cm^3 water/(cm^3 snow × h)
S	effective water saturation $(S_w - S_i)/(1 - S_i)$		cm^3 of (total water-immobile) volume/cm^3 of (pore-immobile) volume
S_i	irreducible water content: irreducible volume of water over pore volume		cm^3 of immobile water volume/cm^3 of pore volume
S_w	total water content: total water volume over the pore volume		cm^3 of total water volume/cm^3 of pore volume
t	time	h	
u	water velocity	cm h^{-1}	cm snow/s
V_{melt}	melting rate	cm h^{-1}	cm^3 of snow volume/(cm^2 of snow × h)
V_{rf}	spraying rainfall rate	cm h^{-1}	cm^3 of water volume/(cm^2 of snow × h)
z	depth ($z = 200$)	cm	
β	$S_i/(1 - S_i)$		
θ	volumetric water content		cm^{-3} of water volume/cm^3 of pore volume
ρ_{ice}	density of ice	g cm^{-3}	g of ice/cm^3 of ice
ρ_w	density of water	g cm^{-3}	g of water/cm^3 of water
ϕ	porosity		cm^{-3} of pore volume/cm^3 of total volume
ω	exchange rate coefficient	h^{-1}	

where ρ_w and μ are the density and viscosity of the fluid, respectively, g is the gravitational acceleration, and k is the permeability of a porous medium. Using mass conservation, the governing equation for one-dimensional water percolation in the snowpack [*Colbeck*, 1972; *Hibberd*, 1984] is

$$\phi(1 - S_i)\frac{\partial S}{\partial t} + \frac{\partial (KS^n)}{\partial z} = 0, \tag{3}$$

where ϕ is porosity, S_i is irreducible water content in the snowpack, z is the depth into the snowpack, and t is time. If the irreducible water is immobile, the water percolation velocity, u, is expressed as

$$u = \frac{KS^n}{\phi(S_w - S_i)} = \frac{KS^{n-1}}{\phi(1 - S_i)}, \tag{4}$$

where S_w is the fraction of total water volume in pore space and $S_w = (1 - S_i)(S + \beta)$, $\beta = S_i/(1 - S_i)$.

[15] Solute transport equations come from the standard mobile-immobile model (MIM). The general governing equations are

$$\frac{\partial (SC_m)}{\partial t} = \frac{\partial}{\partial z}\left(SD\frac{\partial C_m}{\partial z}\right) - \frac{\partial}{\partial z}(uSC_m) + \frac{\omega}{\phi(1 - S_i)}(C_i - C_m) \tag{5}$$

$$\frac{\partial C_i}{\partial t} = \frac{\omega}{\phi S_i}(C_m - C_i), \tag{6}$$

where C_m and C_i are the tracer concentrations in the mobile and immobile water fractions, respectively, ω is the rate coefficient for exchange between mobile and immobile waters, and D is the dispersion coefficient.

2.4.2. Numerical Calculations

[16] Differential equations (3), (5) and (6) were solved numerically. For (3), the spatial derivative was described by the upwind finite difference, and a second-order explicit Runge-Kutta scheme was used for the time domain integration. For equations (5) and (6), the advective component of transport was expressed by the upwind finite difference and the dispersive component by the central difference, and the Crank-Nicolson method was used for the time domain integration.

[17] To solve (3), we assumed that initially $S = 0$; that is, there was no water percolating in the snowpack. This assumption is justified because the discharge was very low owing to the cold weather. The irreducible water content, S_i, was assumed to be 0.05 homogeneously, corresponding to the measured water contents near the base of the snowpack. The hydrological boundary condition at the snow surface equals the flux of water introduced to the snowpack as both rain and snowmelt,

$$KS^n_{surface}\rho_w = V_{rf}\rho_w + (a + b)V_{melt} = V_{rf}\rho_w + V_{melt}[\phi(1 - S_i) \cdot (S_{surface} + \beta)\rho_w + (1 - \phi)\rho_{ice}], \tag{7}$$

where a is the mass of water and b the mass of ice per unit snow volume. The parameter ρ_{ice} is the density of ice, and $\beta = S_i/(1 - S_i)$. The variables V_{rf} (cm rain/hr) and V_{melt} (cm

snow/hr) are the rainfall and melt rates, respectively. The melting rate of snow was calculated from an empirical relationship between melting rate and incoming and outgoing shortwave radiation and air temperature, based on high-frequency measurements (10 min per reading). The calculated melting rate compared well with the observed changes in snow depth during the experiments. At the base of the snowpack, the discharge rate is $KS_{base}^{n}\ \rho_w$, with S_{base} being the S value at the lower boundary.

[18] For chemical tracers, the flux at the snow surface is

$$KS^n\rho_w C_m - D\frac{\partial C_m}{\partial z}a_m = V_{rf}\rho_w C_r + V_{melt}a_i C_i + V_{melt}a_m C_m + V_{melt}bC_{ice}, \quad (8)$$

where a_m and a_i are the masses of mobile and immobile water per unit snow volume, and C_r and C_{ice} are the solute concentrations in the rainfall entering the snowpack and the ice (snow grains) melting at the surface, respectively.

[19] At the bottom, a zero concentration gradient is used,

$$\frac{\partial C_m}{\partial z} = 0. \quad (9)$$

This condition is often used for a system with a finite length, and is based on the assumption that the concentration is macroscopically continuous at the outlet, and that no dispersion occurs outside of the snowpack [*Parlange et al.*, 1992].

[20] The value of D is treated as a function of water velocity such that

$$D = d \cdot u = d\frac{KS^{n-1}}{\phi(1 - S_i)}, \quad (10)$$

where d is the dynamic dispersivity [*Hibberd*, 1984] and has a value of 0.05 cm [*Harrington and Bales*, 1998].

2.4.3. Model Verification

[21] The validity and reliability of the numerical model were evaluated by comparing simulation results with known analytical solutions for simple boundary conditions [*van Genuchten and Wierenga*, 1976], and by testing for conservation of mass of water and tracers, which were both better than 0.1% in all simulations.

3. Experimental Results

[22] On 5 April the surface of the snowpack was covered with 60 cm of new snow that had fallen in the previous four days. Near the snow surface, the temperature was around $-3°$ to $-4°$C and increased with depth to 0°C (because of coexistence of liquid and ice) at about 80 cm below the surface. After the first spray, the entire profile became isothermal at 0°C. Within this top 80 cm, the water content was very low, ranging from 0.03 to 0.06% of the total snow volume. Below this layer, the water content increased to about 1.1% down to a depth of 140 cm from the surface. The bottom 80 cm had even higher water contents with an average of 2.6% (1.3 to 3.5%). It is likely that this bottom layer represents the typical irreducible water content, while near the surface liquid water could be lost by either freezing or upward vapor transport due to cold air temperatures. The average water content increased from 1.1 to 1.9 after the first spray and to 2.8 after the second spray. The bulk density of this layer ranged from 0.10 at the surface to 0.16 at 60 cm depth. A visible coarse layer separated this new snow layer from the older snow underneath. Two additional coarse (granular ice) layers were identified at 100 cm and 170 cm from the surface. The average density of the entire profile was 0.35 ± 0.14 (N = 23), increasing to 0.39 ± 0.10 (N = 22) after the first artificial rainfall, and to 0.43 ± 0.07 (N = 19) after the second storm. Changes in density occurred only near the surface within the new snow layer; the depth of this layer also reduced by the storms.

[23] Tracer concentrations in the unspiked tap water were 0.24 and 0.0 mg/L (below the detection limit) for F^-, and Br^-, respectively. The sulfate concentrations in the artificial rain averaged 9.4 and 8.8 mg/L in the first and second artificial storms, respectively. The average concentrations of F^-, Br^- and SO_4^{2-} in the snow profile were 0.02, 0.0, and 1.1 mg/L, respectively. The average concentrations of the solutions sprayed onto the snow surface were 8.0 mg/L (7.4 mg/L in tank 1 and 8.6 mg/L in tank 2) for fluoride, and 14.6 mg/L (15.9 mg/L in tank 1 and 13.3 mg/L in tank 2) for bromide. Thus the applied F^- and Br^- concentrations were 1 or more orders of magnitude above the background concentrations in the snow and the applied SO_4^{2-} concentrations were about a factor of 8 above background.

[24] Water fluxes and chemical concentrations as a function of time for the rain-on-snow experiments are shown in Figure 1. The two artificial rainstorms are indicated in the input of water fluxes. For each storm, the discharge responded to the rainfall and rose to the level of the input flux. After the storm, water drained gradually from the snowpack. The daily snowmelt also caused the outflow flux to increase; the daily snowmelt pulses are seen as the smaller input and discharge peaks in Figures 1a and 1b.

[25] Tracer concentration time series are shown in Figures 1c–1e, for F^-, Br^- and SO_4^{2-}, respectively. For the first storm, the F^- tracer was measured in the discharge after 130 min. However, owing to instrumental problems, there were no flow data during this time and no chemical samples so that the timing of the hydrological and chemical responses cannot be precisely measured. During the second storm, the discharge flow rate responded 80 min after the onset of the storm and the tracer appeared in the discharge after another 30 min. The concentrations of all tracers in the discharge reached maximum levels close to those in the input water, and then they decreased nearly exponentially as the discharge decreased. The tracer concentrations responded to each change in hydrological conditions, such as melting or another storm. For instance, the concentration of fluoride, which had been applied in the first artificial storm on 5 April, decreased from 6 to 4 mg/L owing to snowmelt on 7 April, and further decreased to nearly zero when the second storm (free from F^-) was generated on 8 April (Figure 1c). The relatively clean water fluxes diluted the tracers from the first storm. The rate of F^- concentration decrease was greater on 8 April than on 7 April, because the second rain-on-snow event had a greater input flux of water than the former natural snowmelt event. The concentration of sulfate also decreased from 6 to 4 ppm in response to the snowmelt on 7 April. However, it increased again with the

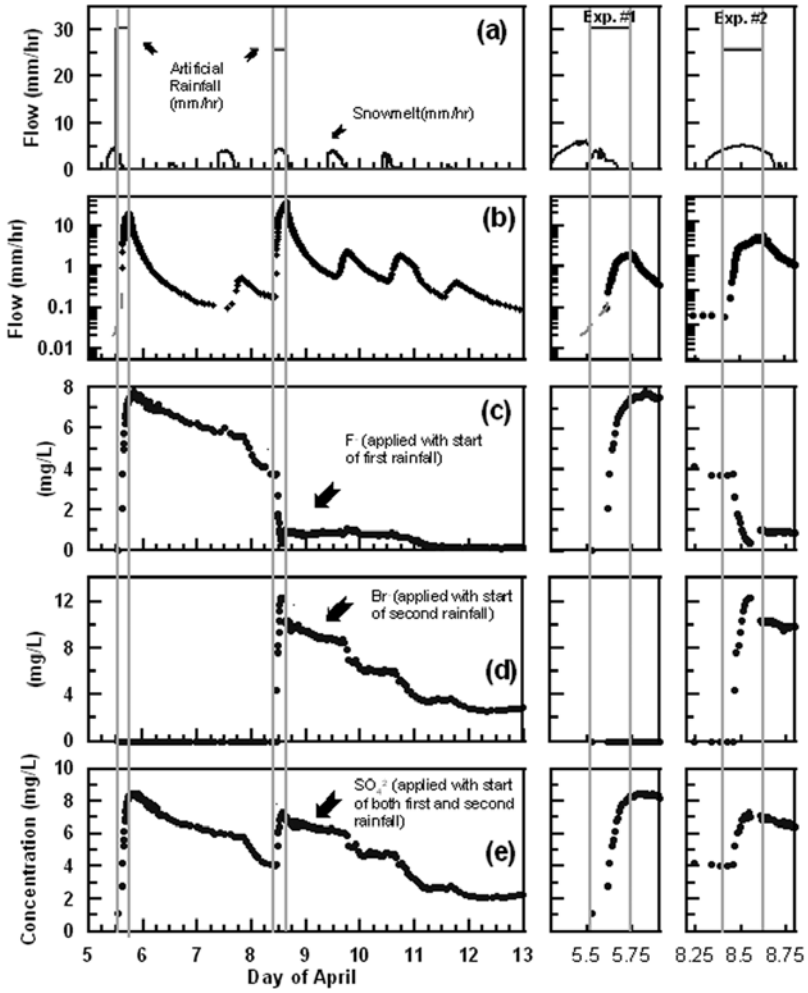

Figure 1. Experimental observations from the two artificial rain-on-snow events, showing (left) the 8-day time series, and (middle and right) the two artificial rain-on-snow events with finer timescales. The thin gray lines represent the beginning and end of each rainstorm. (a) Water input, including the artificial rainstorms, and calculated snowmelt. (b) Water output. The dashed gray line represents no flow data during this time period because of an instrumental problem. In Figures 1c–1e, discharge tracers concentrations from the base of the pack.

second rainstorm on 8 April, because the rainwater contained 9.4 mg/L of sulfate.

[26] During the second storm, the concentration of fluoride first decreased to zero and then went back up to 1 mg/L (Figure 1c). In parallel the bromide tracer that was applied with the second storm increased to ~12 mg/L and then dropped sharply to 11 mg/L (Figure 1d). It seems that nearly pure new water reached the bottom through some fast flow channels before the matrix flow arrived.

[27] The mass balances of water and tracers are illustrated in Figure 2. The total input of water (460 mm) during the 8-day experimental period was greater than the total measured discharge (336 mm) by 37%. Before the onset of the second storm, only 48% of rainwater and 55% of the fluoride tracer had been discharged. Similarly, only 51% of the applied sulfate had appeared in the discharge. This suggests that either some storm water from the first event was retained in the snowpack, or some storm water flowed laterally into the dry snow surrounding the inundated area, or both. The mass balance for the second storm was much better. By 12 April, 100% of the bromide tracer had been measured in the discharge, and 95% of water introduced since the onset of the second storm was recovered. Only 70% of the total fluoride and 79% of the total sulfate (applied in both storms) was collected by 12 April. Converting the sum of the applied fluoride and bromide concentration to moles, then 79 molar percent of the sum of F^- and Br^- was collected in the discharge, which is exactly the same as the sulfate mass balance. Clearly, some water sprayed by the first storm still did not reach the snow pan by 12 April. The measured increase of the water content after the first storm accounted for 21% of the water loss, indicating presence of lateral flow due to either ice layers or capillary flow. However, the complete mass recovery of water and tracers of the second storm suggests that once the surrounding snowpack became wet, the water flow was vertical, and there was no further mass loss by lateral flow. Therefore the mass loss by lateral

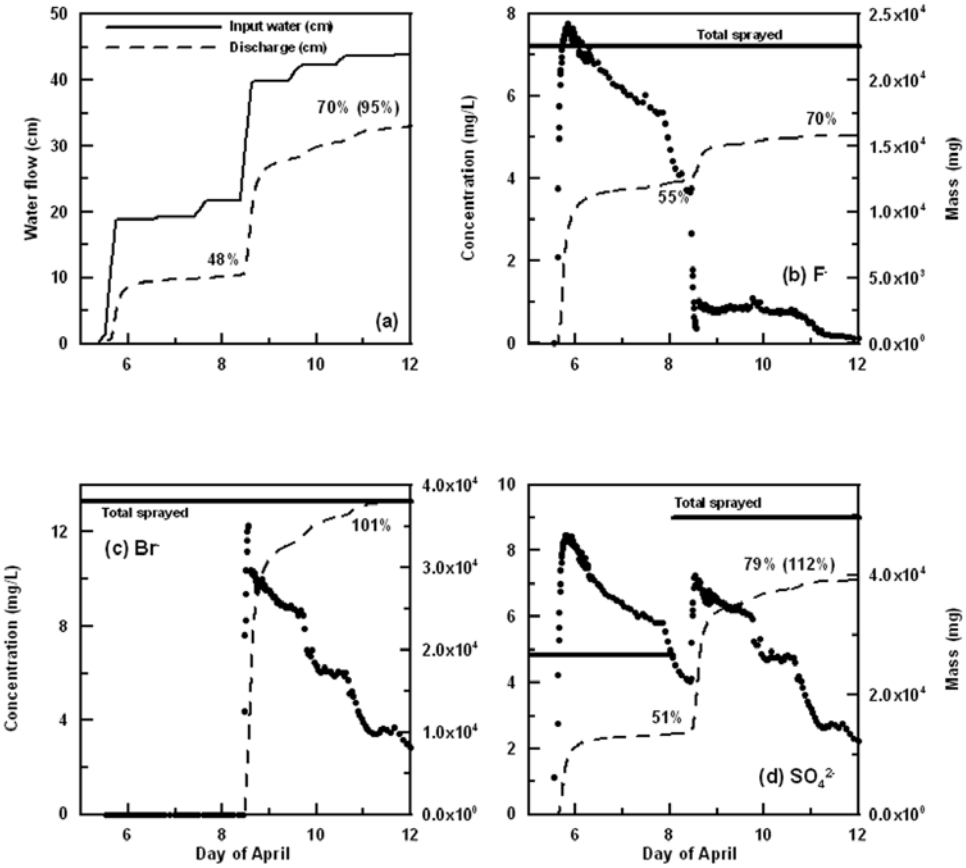

Figure 2. Mass balance calculation of water and tracers. (a) Comparison between input water (centimeters) and discharge collected at the base (centimeters). (b−d) Mass balance calculations of tracers, F^-, Br^- and SO_4^{2-}, respectively.

flow during the first storm was likely caused mainly by capillary suction of the dry snow, rather than by ice layers.

4. Numerical Simulations

[28] We used the flow and solute transport model described in section 2.4 to simulate the experimental observations.

4.1. Water Flow

[29] To simplify the simulation we made the following four assumptions:

[30] 1. Water flow can be described by the one-dimensional vertical flow equation (3), which implies that macroscopic preferential flow introduced by ice layers was insignificant. This assumption was justified by the excellent water and tracer recovery of the second storm, which did not apply to the first storm.

[31] 2. The snowpack was isothermal at the melting point, and the hydrological conditions, including density, porosity, intrinsic permeability, and immobile water content, did not change with time or depth within the snowpack. This was not strictly true, particularly near the snow surface before the first storm where water contents were below the typical irreducible level for wet snow, and the new snow near the surface may have undergone metamorphisms as liquid water percolated through it, altering its the physical properties. However, the assumption is largely valid for the snowpack during the second artificial storm, so that we optimized model parameterization based on the water flow and chemistry data of the second experiment.

[32] 3. Freezing did not occur within the snowpack during the experimental period. This assumption, which is implied by the second assumption, was not invalid before the first storm when the snow near surface was below zero. It was largely valid for the second storm when the measured snow temperature was zero along the entire profile.

[33] 4. To use (3) for the simulation of water flow, we need to know the intrinsic permeability (k), and the exponent (n). We assume that both of these parameters are homogenous throughout the snowpack. We determined the k and n by fitting the model to the observed discharge [*Colbeck and Anderson*, 1982].

[34] We investigated a range of n values in the neighborhood of 3, which is the most commonly used value in the literature [*Colbeck and Anderson*, 1982]. The value of n was varied from 2 to 4 [*Wankiewicz*, 1978] in increments of 0.1, and at each given n, we adjusted k to obtain the best fit. The numerical simulation results for various combinations of k and n values are shown in Figures 3a−3d together with the observed discharge.

[35] It was difficult to select a definition of the "best" fit for this simulation. If a least squares method were used, the best fit was dominated by the second rain-on-snow storm, which had the largest discharge. However, in this simulation the predicted times for the later small peaks were signifi-

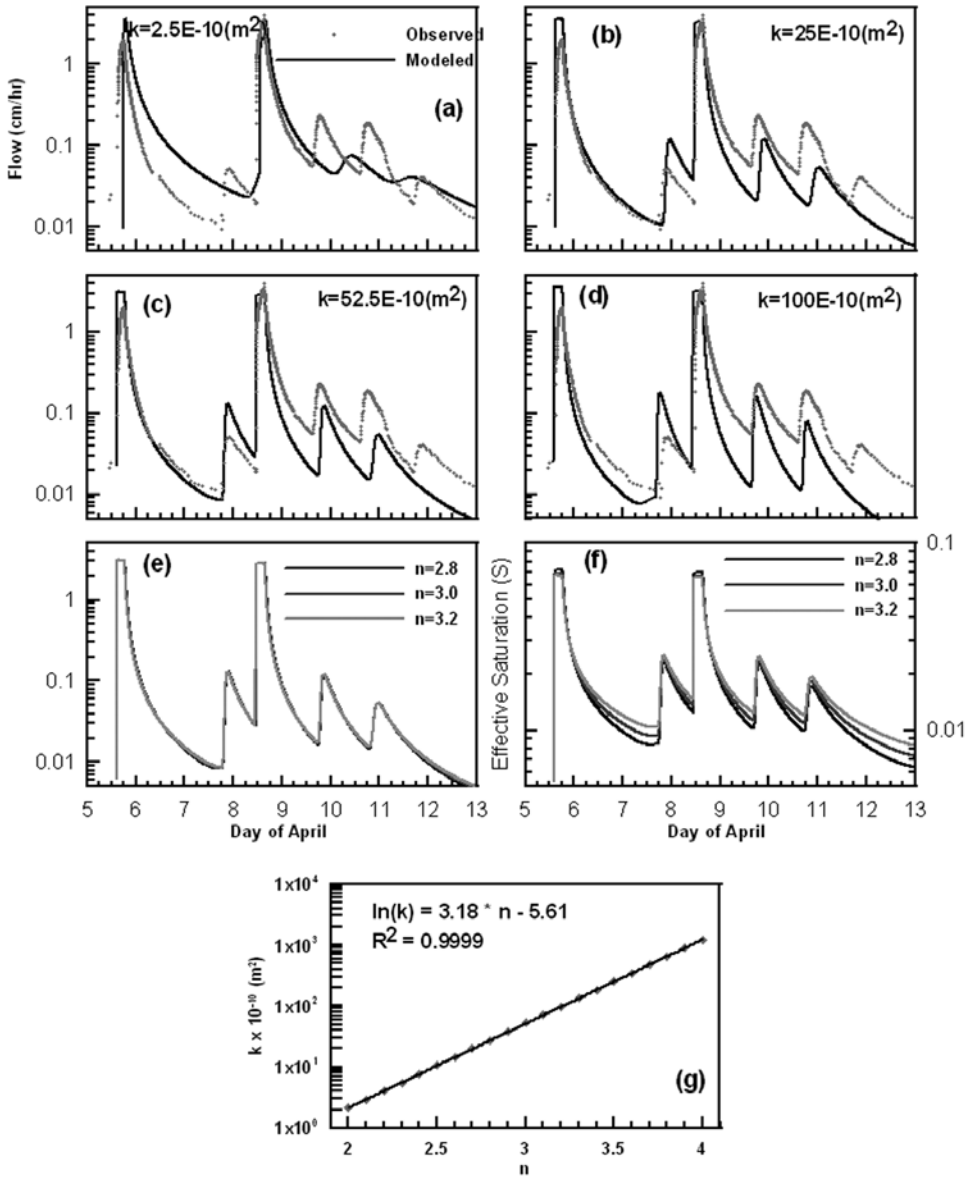

Figure 3. (a–d) Effects of permeability on water flow; Figure 3a is the best fit based on the least squares method, and Figure 3c is the best fit judged by eye and is used in later simulations. (e) The best fit water flow for three different exponents (n values). (f) Effective water saturation for the corresponding simulations in Figure 3e. (g) The relationship between k and n for best fit simulations.

cantly off (Figure 3a). For other best fit criteria, such as a logarithmic least squares, or least squares using the first derivatives of the discharge, the results were similar. Visual examination of a large number of simulations, exemplified by Figures 3b–3d, suggests that Figure 3c ($n = 3$; $k = 52.5 \times 10^{-10}$ m^2) provide the best balance between the size of the peaks and their timing. We consider this simulation the best fit, and we use the flow computed with this combination of n and k in the chemical simulations in section 4.2. We also point out that while the "best" fit simulated the second storm well, it favored a simulated peak for the first storm that is bigger than the measured peak, because the snowpack was dry before the first storm, which was not explicitly considered by the model.

[36] For the range of n values used, the k values that yielded the best fit were systematically related to n, indicating that the best fit k increases exponentially with the assumed value of n (Figure 3g). The goodness of fit is comparable for the entire range of n values, and three examples are shown in Figure 3e for n = 2.8, 3.0, and 3.2. However, the water content, S, corresponding to each of these simulations is different (Figure 3f). During high flow S is low when n is high, while during low flow S is high when n is also high. This nonuniqueness in the simulated water content of the snowpack has an impact on chemical transport, which is affected by both mobile and immobile water contents [*Harrington and Bales*, 1998].

4.2. Chemical Transport

[37] The chemical transport equations (5) and (6) were used for simulations of tracer concentrations in the dis-

charge. The initial mobile water and immobile water were assumed to be free of fluoride and bromide tracers,

$$C_m|_{t=0} = 0, \text{ and } C_i|_{t=0} = 0. \quad (11)$$

The initial sulfate concentration in both mobile and immobile water were assumed to be 1.33 ppm,

$$C_m|_{t=0} = 1.33, \text{ and } C_i|_{t=0} = 1.33. \quad (12)$$

This value was the average sulfate concentration in the fresh snow. The variables used in this calculation are given in Table 1.

[38] A key parameter in the model is the rate coefficient for the exchange between mobile and immobile water, ω. *Harrington and Bales* [1998] used a constant value for ω, while *Feng et al.* [2001] allowed ω to increase exponentially with the effective water content, S. They found that variation of ω was necessary to explain the increase in tracer concentration with increasing water flux. For this experiment, we were unable to simulate the observed temporal variations of tracer concentrations using a fixed ω. This reconfirms that the exchange rate coefficient must vary with hydrological conditions.

[39] Our model uses the assumption that the exchange rate coefficient is directly affected by the flow velocity, such that ω increases linearly with the latter [*Bajracharya and Barry*, 1997; *Griffioen et al.*, 1998; *Schwartz et al.*, 2000; *Haws et al.*, 2004], as one would expect from dispersive mixing,

$$\omega \propto u = \frac{KS^{n-1}}{\phi(1 - S_i)}. \quad (13)$$

[40] The best simulations of fluoride, bromide and sulfate concentrations are shown in Figures 4c, 4d and 4e, respectively, together with the observations. We used $n = 3$ and $k = 52.5 \times 10^{-10}$ (m^2) for simulating water flow, and the exchange rate coefficient was given by $\omega = 3.3 \times 10^{-5}\, u$ (or $\omega = S^2/2.25$). As seen in Figure 4c through 4e, the model simulated all three tracers reasonably well using the same set of parameters. We tried to optimize the model based on the chemical data of the second storm because the model assumptions were largely valid. Some inconsistencies between the tracer simulations and observations are a consequence of inaccuracies in the discharge flow rate simulations. For example, the simulations of both F^- and SO_4^{2-} showed more substantial dilution during the snowmelt event between the two storms than the observations because the simulated discharge flow rate was greater than the observed one. We consider these inconsistencies to be minor, and the model to be apposite to fit the essential features of the observations.

5. Discussion

[41] Given that the model reproduces the water flow and solute transport of our experiments reasonably well, we believe that the model, to the first order, adequately represents the physical processes controlling the behavior of both the water and the tracers in snow. We now use this model to explore how hydrological and chemical conditions can affect solute transport in snow. We have two scientific questions as set up at the beginning of this paper: (1) whether the mobile-immobile water exchange coefficient is necessarily dependent upon the flow velocity and (2) whether the same set of equations can reproduce both positive and negative concentration-discharge relationship. We answer each of these questions in the following two sections.

5.1. Exchange Rate Coefficient (ω) and Pore Water Velocity (u)

[42] As explained in the previous section, the exchange rate coefficient between mobile and immobile waters (ω) is assumed to be proportional to the pore water velocity (u). Figure 5 shows how the tracer concentration changes with various formulations of ω. The hydrological conditions among these simulations are the same as those in Figure 3c. With fixed ω (here $\omega = 1.44 \times 10^{-4}$ hr^{-1} [from *Harrington and Bales*, 1998]), we cannot successfully simulate the variation of the sulfate concentration in the discharge (Figure 5a), particularly in that when discharge decreased after the two storms, the simulated concentration decreased more rapidly than the observed concentration. This is apparent when comparing the simulation in Figure 5a with that in Figure 5d (the best fit).

[43] With a variable ω, the concentrations of mobile and immobile waters can buffer each other (Figures 5b, 5c, and 5d). When the exchange rate is high (e.g., Figures 5b and 5f), the solute contributions from the immobile water make the mobile water concentrations less variable than they otherwise would be, and the mobile and immobile water concentrations become similar (see Figure 5e for immobile water concentration at the base of the snowpack). When the exchange rate is low (e.g., Figures 5c and 5f), the mobile water concentrations are much more variable owing to a lack of buffering from solute delivery by the immobile water. An intermediate value of the rate coefficient (Figures 5d and 5f) provides the appropriate level of communication between mobile and immobile water, yielding a range of solute variation in the discharge similar to the observation.

5.2. Concentration-Discharge Relationship

[44] We used the same model, but changed the boundary condition to produce a regular daily water input at the snow surface (see Figure 6a). We made the input water completely free of tracers, because the snowmelt is usually relatively clean, and we could observe the interaction of solutes in the initial mobile and immobile waters. The snowmelt rate was set to zero so that the depth of snow would not change, and the mobile and immobile water chemistry would not be affected by snowmelt during the numerical experiment. We conducted two simulations. In the first simulation, we examined how solute transport was affected by where the solutes were (i.e., in the mobile versus immobile phase) before the clean water fluxes were introduced. In the second simulation, we examined how the solute distribution within the snowpack might affect the concentration-discharge relationship.

[45] Figures 6a and 6b contain the input and output water fluxes of water for the simulations. Solute concentrations in

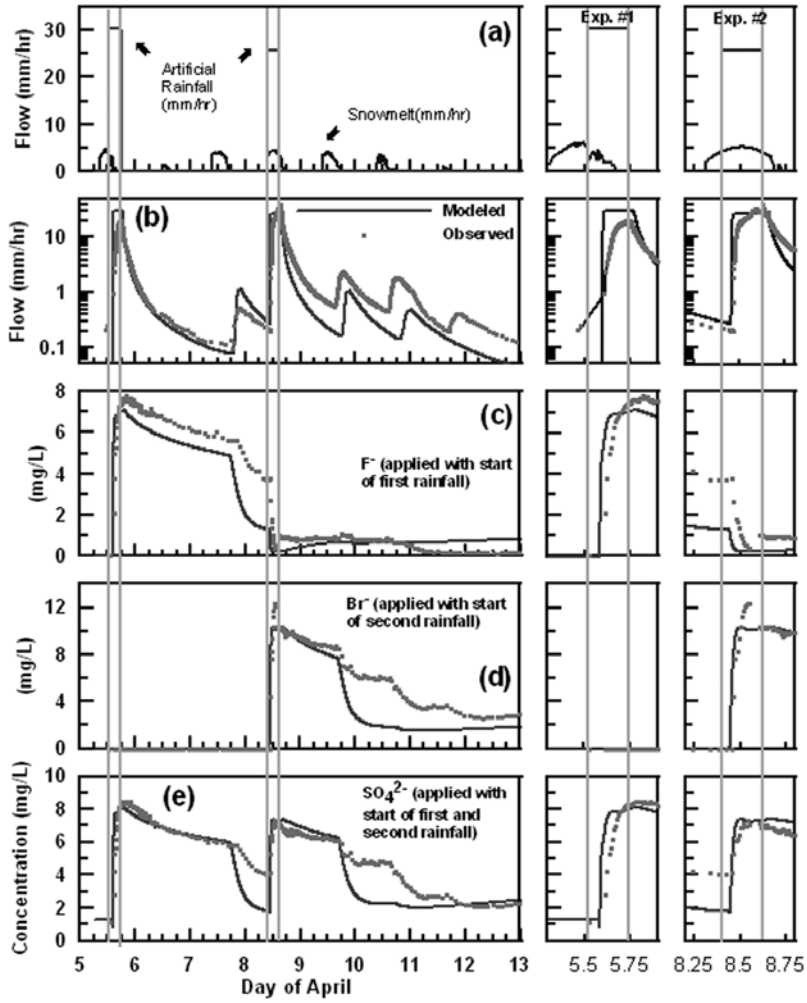

Figure 4. Simulated results (solid lines) with observed data (gray dots). (a) Water input. (b) Water output, with modeling parameters identical to those used in Figure 3c. (c–e) Simulated concentrations of F^-, Br^- and SO_4^{2-} in the discharge, respectively. The exchange rate coefficients used in these simulations is $\omega = 3.3 \times 10^{-5}\, u$ (or $\omega = S^2/2.25$).

the discharge were simulated for two initial conditions, 100 mg/L solute either in the mobile water (Figure 6c) or in the immobile water (Figure 6d). When the solute is present only in the mobile water (Figure 6c), it is eluted from the snowpack very quickly by the daily flux of clean water, resulting in a pattern similar to our observations of stepwise reductions in the F^- and Br^- concentrations after the (second) rain-on-snow storms were shut off. On the other hand, when the solute is initially in the immobile water (Figure 6d), the overall concentration decrease in the discharge is much slower because of limited delivery of the solute in the immobile water to mobile water. In both Figures 6c and 6d, an increase in the water flux generated a decrease in the discharge concentration, indicating a dilution effect of the clean water input.

[46] The solute distribution within the initial snowpack also affects the solute transport by the discharge, particularly the concentration-discharge relationship. In Figure 6e we show the result of a simulation with tracers initially present in the immobile water only in the upper 5% of snowpack near the surface while the rest of the snowpack has clean immobile water. The concentration-discharge relationship is reversed from that of Figure 6d; the two variables are now positively associated.

[47] A positive concentration-discharge relationship was observed by *Feng et al.* [2001] in rain-on-snow experiments, in which rare earth element (REE) tracers were applied to the snow surface prior to the rainstorm. Under this condition, the tracers were contained mostly in the immobile water near the surface, a situation similar to our simulation in Figure 6e. Feng et al. attributed this observation to the fact that high flow would result in a high mobile-immobile water exchange coefficient, and would thus introduce more solutes into the mobile fluid. While this mechanism remains a possibility, we observed a different mechanism causing a positive concentration-discharge relationship in our simulation. When water flow is slow (near-zero velocity), the mobile water near the surface becomes highly concentrated by mobile-immobile water exchange, because it remains in contact with the concentrated immo-

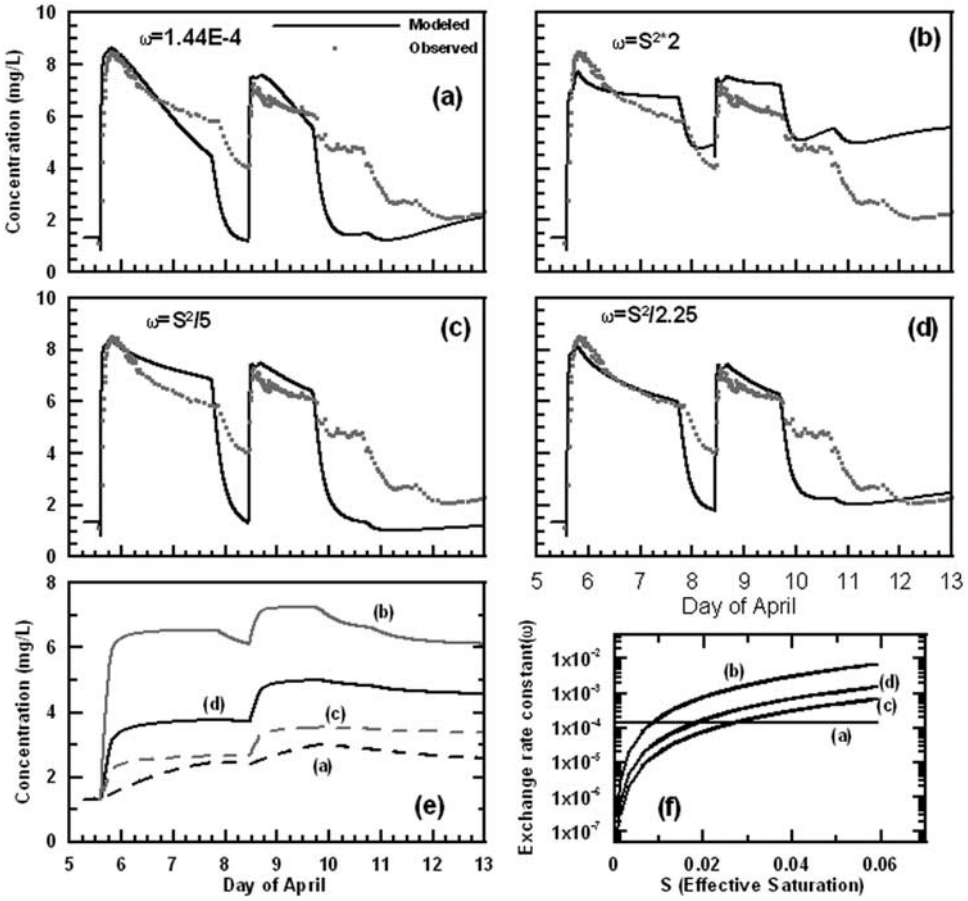

Figure 5. Simulations of the tracer concentration in the discharge using (a) a fixed exchange rate constant and (b−d) different proportionalities between ω and S^2. (e) Tracer concentrations in the immobile water at the base of the snowpack. (f) The dependency of the exchange rate coefficient on the effective water content.

bile water for a relatively long time. When the flow rate increases, this local high-concentration fluid is pushed down through the snowpack and eventually appears at the base more or less in phase with the increase in discharge. On the other hand, when the tracer is in the immobile water throughout the entire column, the mobile water of the whole column becomes concentrated at low flow, and when the advection rate increases near the surface, the mobile water is diluted by the clean input water, producing a negative concentration-discharge relationship.

[48] There are a number of other factors that affect the concentration-discharge relationship. One factor is the depth of snow. Because of the kinematic nature of the water percolation in snow, the water wave travels faster than the water itself [e.g., *Hibberd*, 1984; *Feng et al.*, 2001]. Therefore the tracer plume produced near the surface may fall behind the increase in discharge at the snow base. Other factors may also include more complicated patterns of tracer distribution within the snowpack, and the presence of tracers in the solid phase (ice) itself. For example, if a layer of snow contains high concentrations of tracers, melting of that layer would introduce tracers into the mobile fluid.

[49] *Bales et al.* [1989] observed that solute delivery from a snowpack is affected by where the solutes were located within the snowpack. Our simulations provide a possible explanation for this phenomenon. Complicated concentration-discharge relationships have been observed in stream water in response to a rainfall or snowmelt event [e.g., *Hornberger et al.*, 2001; *Borah et al.*, 2003]. It is possible that mechanisms similar to those we observed in snow may also operate in unsaturated soil on the catchment scale, although additional complicating factors may apply, such as different travel distance for different topographic locations.

6. Conclusion

[50] We conducted two artificial rain-on-snow experiments, with conservative tracers introduced with the rainstorms. These experiments produced a negative concentration-discharge relationship, which was opposite to the tracer experimental results of *Feng et al.* [2001] when tracers were introduced as immobile water near the snow surface.

[51] We developed a model that dynamically links a standard water percolation model with a mobile-immobile model (MIM) to simulate the discharge and its tracer concentrations. The model successfully reproduced the main features of the variations in water fluxes and solute concen-

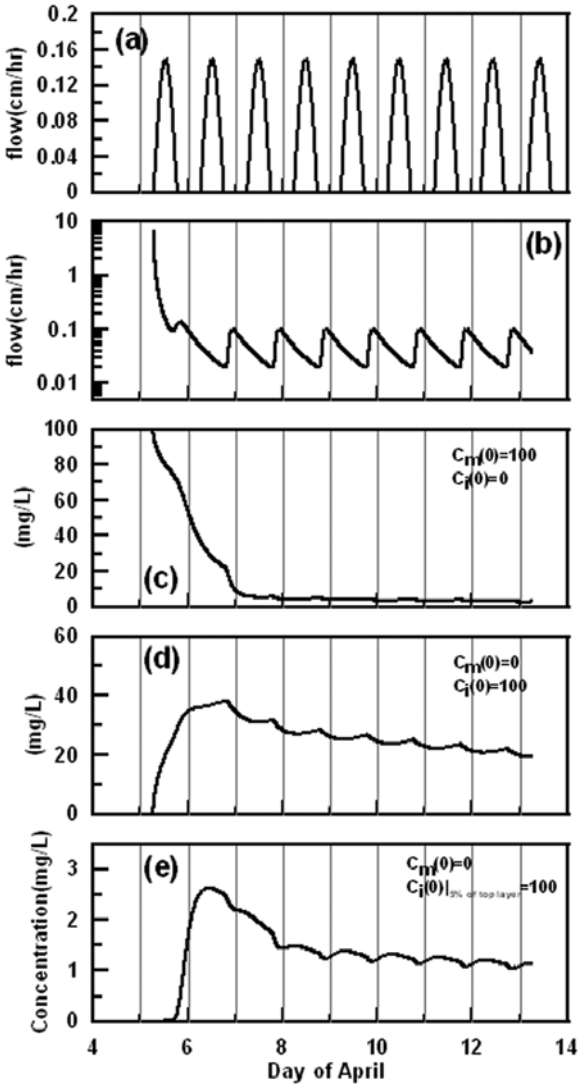

Figure 6. Simulations of solute transport in response to diurnal input water pulses. (a) Daily clean water (as rainwater, not snowmelt) flux as input water to the snow surface. (b) Water discharge generated by the daily pulses of input water. (c) Tracer concentration simulated with the initial condition that all solutes are in the mobile phase. (d) Discharge tracer concentration with the initial condition that all solutes are in the immobile phase. (e) Discharge tracer concentration simulated with the initial condition that solutes are contained in the immobile water of the top 5% of the snowpack. Other than the initial and boundary conditions, all parameters are the same as those used in Figure 4.

tration observed in our experiments. With such a model, the rate coefficient for mobile-immobile water exchange must increase with water flow velocity in order to reproduce the observed tracer fluctuations. We also showed that the concentration-discharge relationship is, at least in part, determined by how chemical tracers are introduced (as mobile versus immobile water) and by how they are distributed in the snowpack (e.g., uniformly throughout in the whole pack versus only near the surface). The physical mechanisms revealed by our simulations and interpretations may also be relevant to solute transport processes in unsaturated soil and may shed light on explanation of concentration-discharge relationships observed from lysimeters and streams.

[52] Our model cannot simulate certain minor features of our experimental data. For example, the model could not reproduce the sharp increase of fluoride and decrease of bromide at the end of the second storm. The sharp changes in F^- and Br^- concentrations probably resulted from preferential flowpaths that delivered the new water to the base of the snowpack before the matrix flow arrived. Our model does not specify such distinct flowpaths. How important such flowpaths are for delivery of natural solutes from snowpack remains to be further investigated.

[53] **Acknowledgments.** This research was partially supported by the National Science Foundation (EAR-9903281, EAR-0111403, EAR 0418809) and by Dartmouth College. We appreciate Roger C. Bales and an anonymous reviewer, whose comments led to significant improvements.

References

Bajracharya, K., and D. A. Barry (1997), Nonequilibrium solute transport parameters and their physical significance: Numerical and experimental results, *J. Cont. Hydrol.*, *24*, 185–204.

Bales, R. C., R. E. Davis, and D. A. Stanley (1989), Ion elution through shallow homogeneous snow, *Water Resour. Res.*, *25*, 1869–1877.

Borah, D. K., M. Bera, and S. Shaw (2003), Water, sediment, nutrient, and pesticide measurements in an agricultural watershed in Illinois during storm events, *Trans. ASAE*, *46*, 657–674.

Colbeck, S. C. (1972), A theory of water percolation in snow, *J. Glaciol.*, *11*, 369–385.

Colbeck, S. C., and E. A. Anderson (1982), The permeability of a melting snow cover, *Water Resour. Res.*, *18*, 904–908.

Feng, X., J. W. Kirchner, C. E. Renshaw, R. S. Osterhuber, B. Klaue, and S. Taylor (2001), A study of solute transport mechanisms using rare earth element tracers and artificial rainstorms on snow, *Water Resour. Res.*, *37*, 1425–1435.

Griffioen, J. W., D. A. Barry, and J.-Y. Parlange (1998), Interpretation of two-region model parameters, *Water Resour. Res.*, *34*, 373–384.

Harrington, R., and R. C. Bales (1998), Modeling ionic solute transport in melting snow, *Water Resour. Res.*, *34*, 1727–1736.

Harrington, R., R. C. Bales, and P. Wagnon (1996), Variability of meltwater and solute fluxes from homogenous melting snow at the laboratory scale, *Hydrol. Processes*, *10*, 945–953.

Haws, N. W., B. D. Das, and P. S. Rao (2004), Dual-domain solute transfer and transport processes: Evaluation in batch and transport experiments, *J. Cont. Hydrol.*, *75*, 257–280.

Hibberd, S. (1984), A model for pollutant concentrations during snow-melt, *J. Glaciol.*, *30*, 58–65.

Hornberger, G. M., T. M. Scalon, and J. P. Raffensperger (2001), Modelling transport of dissolved silica in a forested headwater catchment: the effect of hydrological and chemical time scales on hysteresis in the concentration-discharge relationship, *Hydrol. Processes*, *15*, 2029–2038.

Johannesssen, M., and A. Henriksen (1978), Chemistry of snow meltwater: Changes in concentration during melting, *Water Resour. Res.*, *14*, 615–619.

Parlange, J.-Y., J. L. Starr, M. T. van Genuchten, D. A. Barry, and J. C. Parker (1992), Exit condition for miscible displacement experiments, *Soil Sci.*, *153*, 165–171.

Schwartz, R. C., A. S. R. Juo, and K. J. McInnes (2000), Estimating parameters for a dual-porosity model to describe non-equilibrium, reactive transport in a fine-textured soil, *J. Hydrol.*, *229*, 149–167.

Singh, P., G. Spitzbart, H. Hübl, and H. W. Weinmeister (1997), Hydrological response of snowpack under rain-on-snow events: A field study, *J. Hydrol.*, *202*, 1–20.

Tranter, M., P. Brimblecombe, T. D. Davies, C. E. Vincent, P. W. Abrahams, and I. Blackwood (1986), The composition of snowfall, snowpack and meltwater in the Scottish highlands—Evidence for preferential flow, *Atmos. Environ.*, *20*, 517–525.

van Genuchten, M. T., and P. J. Wierenga (1976), Mass transfer studies in sorbing porous media: I. Analytical solutions, *Soil Sci. Soc. Am. J.*, *40*, 473–480.

Wankiewicz, A. (1978), A review of water movement in snow, in *Modeling of Snow Runoff*, edited by S. C. Colbeck and M. Ray, pp. 222–252, U. S. Army Cold Reg. Res. and Eng. Lab., Hanover, N. H.

Williams, M. W., and J. M. Melack (1991), Solute chemistry of snowmelt and runoff in an alpine basin, Sierra Nevada, *Water Resour. Res.*, *27*, 1575–1588.

A. M. Faiia, X. Feng, J. Lee, and E. S. Posmentier, Department of Earth Sciences, Dartmouth College, 6105 Fairchild Hall, Hanover, NH 03755, USA. (jeonghoon.lee@dartmouth.edu)

J. W. Kirchner, Department of Earth and Planetary Science, University of California, Berkeley, CA 94720, USA.

R. Osterhuber, Central Sierra Snow Laboratory, Box 810, Soda Springs, CA 95728, USA.